Chaotic dynamics of periodically driven rf superconducting quantum interference devices

R. K. Ritala
Research Institute for Theoretical Physics, University of Helsinki, Siltavuorenpenger 20C, SF-00170 Helsinki 17, Finland

M. M. Salomaa
Low Temperature Laboratory, Helsinki University of Technology, SF-02150 Espoo 15, Finland
(Received 28 November 1983)

We present numerical investigations of the intrinsic noise in periodically driven, high-frequency, rf superconducting quantum interference devices (SQUID's) due to the chaotic time evolution of the flux trapped in the superconducting ring. The amplitude and the frequency of the external sinusoidal magnetic flux are the control parameters of the SQUID dynamics. The present work shows in detail how the well-known quasistationary behavior evolves into chaos at high frequencies. A rich structure of subharmonic and chaotic bands is observed in the parameter space. Both intermittent and period-doubling routes to chaos are found; the latter is always preceded by a broken symmetry, and thus the former is the governing one for small amplitudes. We also discuss the experimental observability and manifestations of multiply periodic and chaotic SQUID response. In particular, the usual staircase dependence of the absorbed hysteresis power on the amplitude of the external flux is shown to be broken in a characteristic way for each main subharmonic. Thus we propose that simple dc measurements can detect important properties of the nonlinear SQUID dynamics.

I. INTRODUCTION

The recently introduced modern theory of chaos[1] in deterministic systems has pointed out important new sources of intrinsic noise in varied physical realizations of nonlinear dynamics. The mathematics of the period-doubling route to chaos[2,3] has already been studied in great depth, and this route has been observed in several experiments.[4,5] The intermittent route to chaos is also known to display universal behavior with characteristic scaling laws.[6,7] However, until now most studies have only been carried out on discrete one-dimensional dynamical systems. We note that continuum dynamics can always be considered discretized through the use of Poincaré sections (or return maps), and that work on the role of higher dimensions has only quite recently commenced.[8]

The simplest physical system to display chaotic behavior is a driven pendulum under linear friction.[9] A mathematical analog model of this is the current-driven Josephson junction, for which the scaling behavior predicted by Feigenbaum's universal theory of period-doubling sequences has been observed.[10] Moreover, the anomalous noise rise in parametric amplifiers[11] has been interpreted in terms of the chaotic response of the junction.[12] Computer simulations[13] as well as some analytical approaches[14] have revealed other interesting physical phenomena, which are also manifestly due to nonlinear origin: running solutions, intermittency,[15] and solutions which break the symmetry of the governing dynamics.

In this paper we present numerical investigations of intrinsic noise within the resistively-shunted-junction (RSJ) model of a driven rf-SQUID magnetometer (SQUID denotes superconducting quantum-interference device): a superconducting loop closed with a Josephson junction in an oscillating external magnetic field; see Fig. 1. We consider in detail the underdamped high-frequency operating regime, which is of particular interest for the nonlinear dynamics. In addition to our first report[16] on the subharmonic and chaotic states of the RSJ model of the SQUID, there recently appeared another paper[17] on chaos in SQUID's, where the results agree with ours. The present paper concentrates on a detailed description of the phase-space structure, and we consider, in particular, the observability of the predicted nonlinear phenomena and the degree of their universality in real SQUID magnetometer experiments.

In Sec. II we outline the RSJ model and present results of our numerical work on the driven rf-SQUID dynamics. The external field is assumed to vary periodically with a frequency comparable to the Josephson plasma frequency. The systematics underlying the phase-space structure, with several chaotic and subharmonic regimes, is

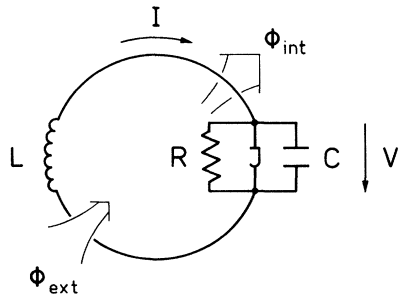

FIG. 1. RSJ equivalent circuit for a rf SQUID. Here V, R, and C are the voltage, resistance, and capacitance across the Josephson junction, I is the circulating current, and L is the self-inductance of the SQUID ring. The internal magnetic flux trapped in the superconducting ring is ϕ_{int}, while ϕ_{ext} abbreviates the external driving flux.

described. We also find solutions with nonvanishing averaged internal flux even if the time average of the driving field vanishes. We emphasize that the appearance of such a spontaneously magnetized state is a consequence of dynamically broken symmetry. Our work also demonstrates an inherent connection between even subharmonics and the broken symmetry. We therefore suggest that the readily observable SQUID magnetization could serve as a useful indication of the broken-symmetry state in actual experiments. We also discuss the effects due to a small external dc flux ("dc bias") on the structure found in the symmetric case. In Sec. III we briefly summarize the known results on the scaling theory of intermittency, and illustrate the appearance of this route to chaos in the rf SQUID. The role of intermittency as a source of intrinsic noise in a SQUID is discussed. The equivalent noise temperature is derived, and the observability of intermittent evolution is studied in the presence of an external noise source, such as a finite temperature. In Sec. IV we discuss, in a similar manner, the period-doubling sequence, emphasizing the aspects of observability. However, in the latter section we concentrate on the simultaneous occurrence of the broken symmetry and the 2^n-subharmonic limit cycles.

The SQUID dynamics we describe is difficult to observe experimentally, principally because the characteristic frequencies of the system are of the order of the Josephson plasma frequency ($\omega_J \sim 10^{12}$ Hz). The usual measuring configuration involving a driving circuit and the observing tank circuit are probably inaccessible for the interesting SQUID dynamics. Also, the tank circuit is likely to become too mixed for the relevant features to be measurable. In Sec. V we present results on the power absorbed by the SQUID from the driving field; this is an easily measurable dc property. As one sees in Fig. 2, the dependence of the internal flux on the applied flux is hysteretic. Hence there is power absorbed during each cycle of the driving field. For the well-known overdamped quasistationary SQUID behavior, the dependence of the absorbed power on the amplitude of the external field has the typical staircase structure displayed in Fig. 3. In the presence of chaos or subharmonic solutions, the SQUID

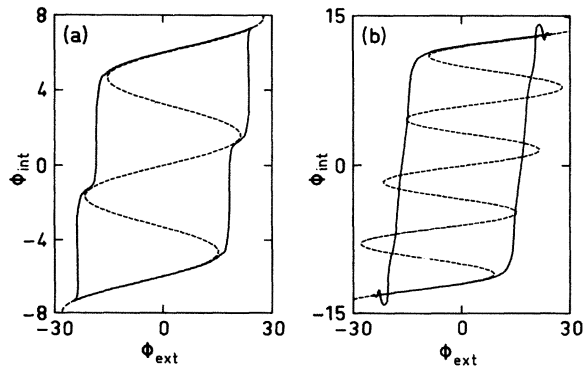

FIG. 2. Internal flux ϕ_{int} enclosed by the SQUID ring as a function of the sinusoidally varying external flux ϕ_{ext} applied at a low frequency ($\omega_D = 0.0001\omega_{res}$) and with the amplitude $A = 27$. Both ϕ_{int} and ϕ_{ext} are in units of $\phi_0/2\pi$, where ϕ_0 is the flux quantum. (a) Critical damping with $\beta_C = 0.25$. (b) The weakly damped case $\beta_C = 5$.

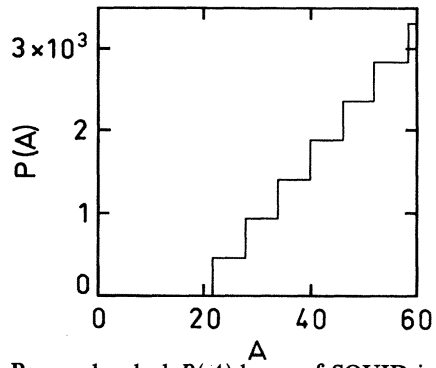

FIG. 3. Power absorbed $P(A)$ by an rf SQUID in the overdamped quasistationary mode of operation as a function of the amplitude of the external driving flux A for $\beta_L = 20$ used in the present paper.

response changes in an essential way and becomes much more complicated. Specifically, we find a typical behavior for each main subharmonic, i.e., periods 2, 3, and 5. We also suggest experiments on this breakdown of the staircase structure as an easy alternative for complicated dynamical measurements to detect chaos in SQUID's.

We end this paper with a short discussion on further important aspects concerning the possible limitations of the present model calculations. We conclude that the SQUID is an interesting nonlinear device which is found to display varied chaotic response, and which is readily accessible for experimentation.

II. EVOLUTION EQUATION AND NUMERICAL RESULTS

A. rf-SQUID model

According to the Stewart-McCumber [the resistively-shunted-junction (RSJ)] model[18] for an rf SQUID, the current I flowing in the SQUID ring is given by[19]

$$I = \frac{\phi_{ext}(t) - \phi_{int}(t)}{L} = C\frac{dV}{dt} + \frac{V}{R} + I_c \sin\left[\frac{2\pi\phi_{int}(t)}{\phi_0}\right], \quad (1)$$

where C, R, and I_c are the capacitance, resistance, and critical current of the junction, and L is the inductance of the ring. The voltage across the junction is denoted with V, and $\phi_{int}(t)$ and $\phi_{ext}(t)$ are the internal and external magnetic fluxes.

The voltage V is related to the internal flux through the Josephson equation:

$$V = \frac{d\phi_{int}}{dt} . \quad (2)$$

The above pair of equations may be cast into the dimensionless form,[16]

$$\beta_C \frac{d^2\theta}{d\tau^2} + \frac{d\theta}{d\tau} + \sin\theta + \frac{1}{\beta_L}\left[\theta - \frac{2\pi\phi_{ext}(\tau)}{\phi_0}\right] = 0 , \quad (3)$$

where $\theta = 2\pi\phi_{int}(\tau)/\phi_0$, and the McCumber parameters are

$$\beta_C=\frac{2\pi}{\phi_0}I_cR^2C,\quad \beta_L=\frac{2\pi}{\phi_0}LI_c\ . \tag{4}$$

In Eq. (3) the dimensionless time variable $\tau=RC\omega_J^2t$, where the Josephson plasma frequency ω_J is given by

$$\omega_J=\left[\frac{2\pi}{\phi_0}\frac{I_c}{C}\right]^{1/2}\ . \tag{5}$$

The low-amplitude oscillations of an rf SQUID are governed by two time constants: the damping rate $2\beta_C$ and the natural resonance frequency,

$$\omega_{\rm res}=\frac{[(1+1/\beta_L)4\beta_C-1]^{1/2}}{2\beta_C}\ . \tag{6}$$

We note that Eq. (3) is an analog to a classical particle of mass β_C moving under linear friction in a potential displayed in Fig. 4 and driven with a force proportional to the external flux.

In order to enhance the chaotic behavior, the parameters should be chosen such that (i) more than one local minimum of the potential exists, and (ii) the system is underdamped. Note that in the limiting case $\beta_L\to\infty$, Eq. (3) reduces to pure Josephson-junction dynamics, for which chaotic behavior is known to occur. The additional harmonic envelope of the potential excludes the finite-voltage running solutions, which are obtained in Josephson junctions.

We found that convenient values for the McCumber parameters are $\beta_C=5$ and $\beta_L=20$. These correspond in practice to the circuit parameters, for example, $I_c=5\ \mu$A, $C=0.1$ pF, $R=50\ \Omega$, and $L=1$ nH. The values of β_C and β_L are kept fixed, for simplicity, throughout this paper. The variation with these parameters has been discussed in Ref. 17.

The quasistationary solution of Eq. (3) is well known:[19] When the external field is varied sufficiently slowly and the system is overdamped, the SQUID responds to the external field smoothly, except for points where the minimum of the instantaneous potential of the SQUID becomes unstable [cf. Fig. 2(a)]. However, an underdamped (though slowly driven) SQUID displays rather unpredictable properties: When the instantaneous potential minimum loses stability, then instead of the increase or decrease of just one flux quantum in the SQUID ring, the exchange of several quanta is possible. In fact, for the parameter values (β_C,β_L) chosen in this paper, the lowest quasistationary solution is the double-quantum loop in Fig. 2(b).

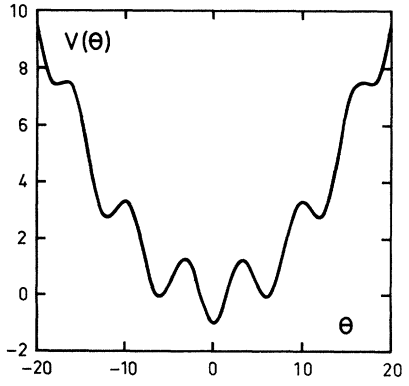

FIG. 4. Effective potential $V(\theta)$ as a function of the phase difference θ of the superconducting order parameter across the weak-link Josephson junction. The dc flux is zero, and the McCumber-parameter value $\beta_L=20$ is used.

B. Phase space

Here we present general results of our numerical investigations of the rf-SQUID dynamics, represented by Eq. (3). The external field is assumed to vary sinusoidally

$$\frac{2\pi\phi_{\rm ext}(\tau)}{\phi_0}=A\sin(\omega_D\tau)\ , \tag{7}$$

where the driving frequency ω_D is taken to be comparable to the Josephson plasma frequency ω_J [and hence also to the resonance frequency $\omega_{\rm res}$ in Eq. (6)]. The control parameters for the phase space discussed below are the amplitude A and the frequency ω_D of the external driving flux.

We have integrated Eq. (3) numerically with the use of the Adams method. The initial conditions were chosen as $\theta(\tau=0)=\dot\theta(\tau=0)=0$. The transients were allowed to die out in 500 periods of the driving field. Then the time evolution of the phase difference over the junction was determined typically for some additional 700 periods of the driving field. This time series was analyzed with the fast Fourier transform (FFT). Some eight points per period were recorded. A supplementary program was used to locate the subharmonic peaks from the power spectra; thus the multiperiodicity of the trajectory could be determined at ease.

The results of these investigations are collected in Fig. 5(a). The subharmonic and chaotic regimes display an extremely delicate structure of bands. The resolution in this diagram is a grid of one dimensionless unit in the A direction and $0.05\omega_{\rm res}$ in the ω_D direction. On a yet finer scale one would see more details as discussed below in Sec. V. The multifurcation diagram presented in Ref. 16 (cf. Fig. 10) is located in this graph along the line $\omega_D=\omega_{\rm res}$. Here we shall generally concentrate on the lower frequencies, since for $\omega_D>\omega_{\rm res}$ the results are found to be similar to the ones reported previously. The most prominent feature in Fig. 5(a) is the occurrence of a pair of bands terminating at $\omega_D\cong0.3\omega_{\rm res}$. These describe one-quantum jump processes which are absent in a slowly driven case, Fig. 2(b). The local potential minimum, which the system occupies, becomes unstable, and the SQUID starts decaying towards the lowest-energy state. However, due to the fast sweep the double-quantum process is not completed (which would then be stopped by friction), but rather reaches only the nearest minimum. This is because the decay time is larger than or comparable with the time required to essentially change the instantaneous potential. The detailed interplay of the decay time and the amplitude and the frequency of the driving field determines which of the n-quantum processes is stable.

A notable feature in Fig. 5(a) is the occurrence of one-quantum processes at high frequencies well below the stat-

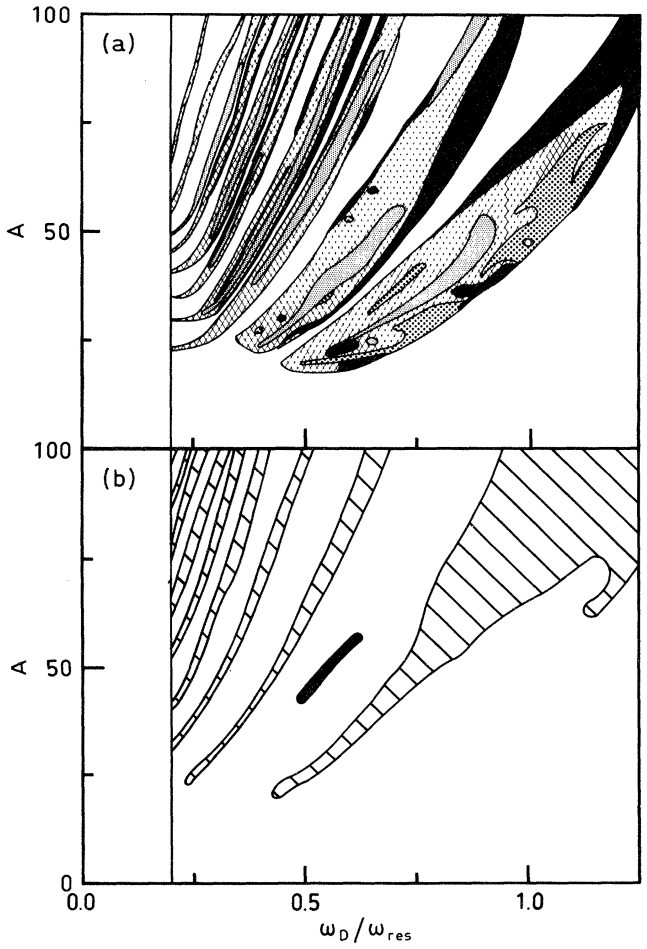

FIG. 5. Phase structure of the driven rf-SQUID dynamics in the ω_D-A plane. (a) The subharmonic and chaotic regimes. Black region: 2^n. Finely dotted region: 3×2^n. Heavily dotted region: 5×2^n. Cross-hatched region: chaos. (b) The regions of broken (hatched region) and "superbroken" (black region) symmetry.

ic threshold value $A=21.6$. The driving field amplifies the intermediate amplitude oscillations for a matching range of frequencies $\omega_D \lesssim \omega_{res}$. This resonance pumping leads to intermittency, as is discussed in Sec. III.

The rich subharmonic structure of the n-quantum bands is due to two different origins: (i) bifurcation (the orbit loses its stability), or (ii) the boundary of the basin of attraction for the orbit moves across the initial-condition point as the control parameter is varied. In the first case some general features are expected, especially as chaos is obtained through bifurcation(s). However, the nonuniversal modifications of the basin of attraction in the second case are unpredictable and essentially depend on the particular system. We trust that these two mechanisms are distinguishable by physical arguments, and therefore we did not compute the stability (i.e., the Lyapunov exponent) of the orbits under consideration.

Figure 5(b) illustrates the control parameter values for which orbits with broken symmetry exist. These regions lie in the gaps between the two split chaotic subbands of n-quantum processes in Fig. 5(a). Between the adjacent n- and $(n+1)$-flux-quantum bands, the orbits are symmetric, except for a small special area above the upper one-quantum subband.

In order to explain the change in the behavior of the rf SQUID upon increasing the amplitude A of the driving field, let us consider the orbits for $\omega_D=0.5\omega_{res}$ in the vicinity of and inside the one-flux-quantum subbands. For low amplitudes, below the first band, the phase difference oscillates around the lowest minimum of the potential, see Fig. 6(a). For a larger amplitude the external field pumps the SQUID sufficiently effectively, such that the lowest potential barrier is crossed. However, this occurs in a rather irregular manner: The SQUID predominantly occupies the lowest minimum, but bursts of one-flux-quantum exchanges occasionally interrupt the time-evolution in Fig. 6(b). This is the intermittently chaotic regime. For larger values of A, the orbits show broken symmetry, such as in Fig. 6(c). In this case the external drive provides sufficient energy for the SQUID to regularly exchange single flux quanta, but in a nonsymmetric way. Consequently, the SQUID is dc magnetized. We refer to this phenomenon as a half-quantum process, in contrast to the quasistationary mode of SQUID operation, in which integer numbers of flux quanta symmetrically enter and leave the SQUID ring during one period of the driving field. Note that no true fractal quantum processes occur, but the averaged flux through the ring is one-half of the flux quantum. A Feigenbaum sequence separates the chaotic and the broken-symmetry regimes in a way similar to that found[16] for $\omega_D=\omega_{res}$ (see also Fig. 10).

The upper chaotic subband is a symmetric one, but an orbit belonging to it does not quite complete a full one-quantum exhange; see Fig. 6(d). The gradual transition from the broken-symmetry regime into the upper chaotic subband again takes place through a Feigenbaum period-doubling cascade. For yet larger amplitudes, the external field finally furnishes the SQUID with sufficient energy to complete a one-flux-quantum exchange process; see Fig. 6(e). The emergence of this new fundamental solution thus had a complicated preceding sequence of intermediate stages from $A=18.5$–43.0. In contrast, for the slowly driven rf SQUID one has a discontinuous transition at $A_c=A_c(\beta_L)=21.6$ from one fundamental solution to another.

All the above-described qualitative features are also evident in each of the higher n-quantum bands, although the bands become narrower. However, the particular feature of "superbroken" symmetry [the black area in Fig. 5(b)] is associated with only the one-quantum band. In this case the SQUID oscillates between the states with 0 and 2 flux quanta; see Fig. 6(f).

A measurement of the predicted dc magnetization of the ac-driven SQUID would constitute an interesting experiment on the nonlinear SQUID dynamics. It appears easy to carry out, since no tank circuit is necessary, and would serve as a useful test of our results, and therefore, also of the applicability of the RSJ equation of time evolution (3) in connection with the high-frequency operation of rf SQUID's.

The above considerations have neglected external noise sources. Thermal motion may cause transitions between

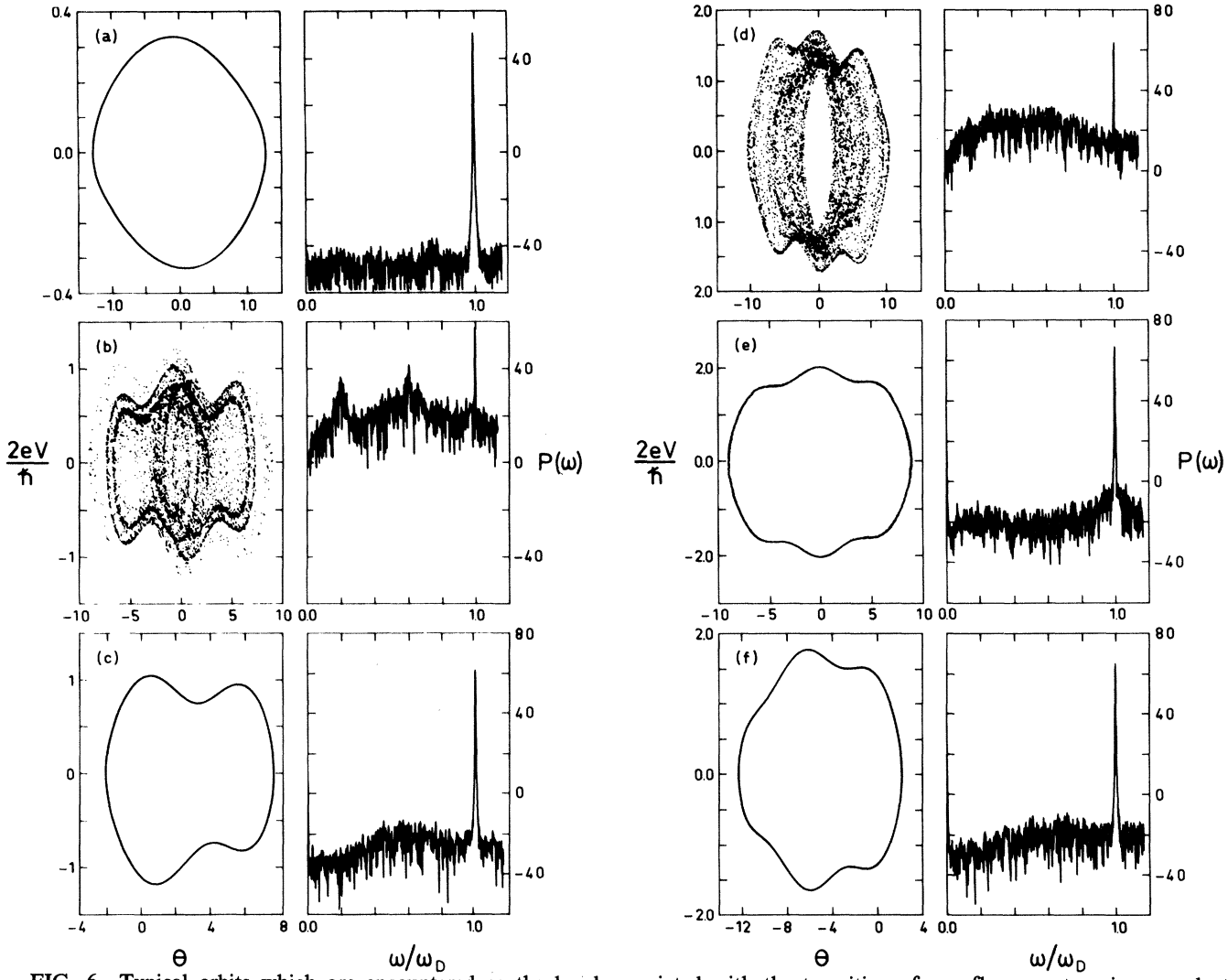

FIG. 6. Typical orbits which are encountered as the band associated with the transition of one flux quantum is crossed at $\omega_D = 0.5\omega_{\rm res}$. (a)—(c): lower subband; (d)—(f): upper subband. Shown on left-hand side are the Lissajous figures of $\dot{\theta}(t)$ vs $\theta(t)$ and on the right-hand side the subharmonic Fourier power spectra $P(\omega)$ of the voltage across the rf-SQUID junction. (a) Phase-locked zero-quantum state at $A = 17.0$; (b) chaotic orbit in the lower band at $A = 22.0$; (c) state with broken symmetry and period one at $A = 25.0$; (d) chaotic state in the upper one-quantum band at $A = 37.5$; (e) phase-locked symmetric one-quantum state at $A = 48.0$; (f) an orbit with "superbroken" symmetry for $A = 44.0$.

different stable limit cycles by activating the flux enclosed in the SQUID or the voltage of the junction across the boundary between two different basins of attraction. This process is important, especially during a measurement of the dc-magnetized regimes in the phase diagram. This is because the occurrence of a nonsymmetric stable orbit $(\theta(t), \dot{\theta}(t))_{\rm ns}$ implies, due to the symmetry of the potential, the existence of another orbit $(-\theta(t), -\dot{\theta}(t))_{\rm ns}$. The time-averaged magnetization in the presence of external noise may thus appear to vanish even in the nonsymmetric regime. For the broken-symmetry states to be observable, the temperature must be sufficiently low, such that the thermal transition rate ω_T obeys

$$\omega_T \ll \omega_D \ . \tag{8}$$

Numerical studies of ω_T are rather time consuming; at present we are not able to give estimates for it.

A static external dc bias may appear as another source of error in experiments. Since a low-frequency background field is likely to appear, we write, instead of Eq. (7),

$$\frac{2\pi\phi_{\rm ext}(\tau)}{\phi_0} = A\sin(\omega_D\tau) + B \ . \tag{9}$$

Here B is a symmetry-breaking field. We recall from the quasistationary case in an overdamped SQUID that a small external bias term will only split the transition from an n- to $(n+1)$-quantum state. Broken-symmetry orbits appear in the gap. For the high-frequency-driven SQUID the transition is already diffuse. Therefore, we conclude (and numerical investigations support this) that the principal effect of the dc term is to broaden the area of the broken-symmetry gap and the two chaotic subbands. Provided that the pairs of the n- and $(n+1)$-quantum bands

are not overlapping, the structure of the solutions remains unchanged. The condition for overlapping is

$$(4n+1)\frac{\pi}{2}+\epsilon<B<(4n+3)\frac{\pi}{2}-\epsilon\,, \tag{10}$$

where ϵ is a small number. The value of external dc bias may be restricted such that no overlapping occurs.

III. INTERMITTENCY IN rf SQUID's

The concept of intermittency was first introduced by Pomeau and Manneville.[20,21] Intermittency refers to a reverse tangential bifurcation: the coalescence of a stable and an unstable orbit, which results in a chaotic motion. They also suggested that intermittency exhibits universality with characteristic critical exponents. The scaling theory of intermittency was developed by Eckmann *et al.*,[22] Hu and Rudnick,[6] and Hirsch *et al.*[7] These authors also considered the effects of external noise on scaling.

Intermittency is characterized by laminar (regular) time-evolution, which is interrupted by bursts. A discrete mapping that describes the main features of intermittency is

$$\theta_{n+1}=\theta_n+b\,|\,\theta_n\,|^z+\epsilon=f(\theta_n)\,, \tag{11}$$

where b, z, and ϵ are parameters. Let us assume that b and z are fixed, and let ϵ be small. Then for $\epsilon<0$, the dynamics defined by Eq. (11) possess two fixed points [which are defined as the solutions of $\theta^*=f(\theta^*)$], a stable and an unstable one. For ϵ tending to zero, the distance between the fixed points diminishes, and for precisely $\epsilon=0$, a single marginally stable point $\theta^*=0$ survives. For positive ϵ, there are no fixed points, and the time evolution is chaotic. However, the system remains in the vicinity of the point $\theta=0$ (the laminar time evolution) for a prolonged time, before diverging away.

The average duration of the laminar evolution obeys the following scaling law:[6,7]

$$t_{\rm lam}\sim\epsilon^{-(1-1/z)}\,, \tag{12a}$$

while the duration of the bursts is independent from the value of the control parameter ϵ. If we were to add a Langevin noise term to the right-hand side of Eq. (11), the mean square of the noise, σ^2, enters the scaling laws as a new relevant parameter. The duration of the bursts is still independent of the parameters, but the laminar time now scales as

$$t_{\rm lam}\sim\epsilon^{-(1-1/z)}T_{\pm}(\sigma/\epsilon^{(z+1)/2z})\,, \tag{12b}$$

where $T_{\pm}$ represent the scaling functions given in Ref. 22. Note that the parameter z enters the scaling exponents, and it thus determines the universality class of the problem. In applying (12a) or (12b) for a complicated model, one thus implicitly assumes that varying the control parameter only changes ϵ and not z, an assumption which need not hold true. This would result in a modification of the critical exponents.

Figure 7 illustrates the time development of the internal flux after the initial transients for three different values of A at $\omega_D=0.5\omega_{\rm res}$. Characteristic intermittent behavior is found. The external flux pumps the SQUID beyond the potential barrier separating the lowest minimum from the state with one flux quantum. This burst terminates when the phase of the external flux matches the phase of the internal flux, whereby the flux quantum is emitted. Increasing the amplitude A provides more energy to the SQUID, and serves to make the absorptions and emissions of flux quanta increasingly frequent. Finally, as the time scale of the laminar motion becomes of the same order as the period of the external flux, the motion appears fully chaotic.

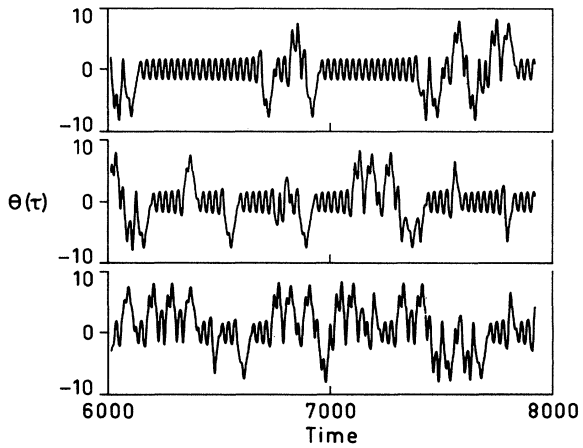

FIG. 7. Intermittent time evolution of the phase difference across the junction above the onset of chaos for $\omega_D=0.5\omega_{\rm res}$. From top to bottom: $A=18.5$, $A=18.6$, $A=18.8$.

Similar changes of stability are observed when the band associated with one flux quantum is approached from above. However, whenever the chaotic bands are approached from the broken-symmetry orbits, intermittency does not appear. Moreover, we have observed that in this respect the structure of the higher n-quantum bands duplicated that of the one-quantum band.

Using the data at $\omega_D=0.5\omega_{\rm res}$, we have determined the

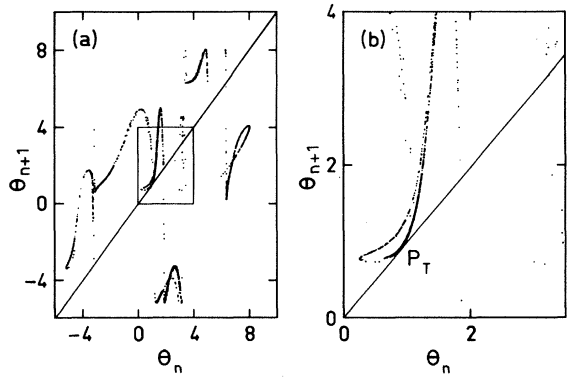

FIG. 8. Return map $\theta((n+1)T_D)=F(\theta(nT_D))$ for the phase difference across the junction. (a) In general, F is a multivalued mapping. (b) However, near the point P_T of tangential contact, the return map is a simple function describable with Eq. (11). This return map is more complicated than that presented in Ref. 17, essentially because the area of the universal part of the map is small, and thus the back-folding part of the mapping is effectively two dimensional.

critical exponent associated with the laminar evolution time, and thus we have also estimated the parameter z which determines the universality class. Figure 8 displays the return map for the internal flux at $\omega_D=0.5\omega_{\rm res}$ and $A=18.5$. The point P_T of tangential contact is responsible for the intermittency observed in Fig. 7. The estimate for the critical exponent z can be obtained by comparing such return maps with the dynamics described by the discrete mapping in Eq. (11). The somewhat large error bars in the value $z=2.5\pm0.5$, that we obtain, may be ascribed to our possibly having determined the critical exponent somewhat away from the critical region. We found no deviations in z when ω_D and A were varied along the intermittency transition line. Hence the intermittent behavior seems universal for the rf SQUID. However, numerical accuracy somewhat limits the possibility to detect small changes in z (the value $z=2$ is the expected result).

Let us now turn to consider effects due to thermal noise on the intermittent route to chaos from the prospective experimental point of view. We add a Langevin noise term with zero average to the equation of SQUID dynamics:

$$\beta_C\ddot{\theta}+\dot{\theta}+\frac{1}{\beta_L}\theta+\sin\theta=\frac{A}{\beta_L}\sin(\omega_D\tau)+\xi(\tau)\ , \tag{13a}$$

where $\xi(\tau)$ represents Gaussian noise with the standard deviation

$$\int_{\tau}^{\tau+\Delta\tau}d\tau d\tau'\langle\xi(\tau)\xi(\tau')\rangle=\frac{2\pi k_BT}{I_c\phi_0}\Delta\tau\ . \tag{13b}$$

Let us integrate Eq. (13a) over the unit period of the applied field in order to construct the return map

$$\begin{bmatrix}\theta((n+1)T_D)\\ \dot{\theta}((n+1)T_D)\end{bmatrix}=\vec{F}(\theta(nT_D),\dot{\theta}(nT_D))+\vec{\xi}(n)\ . \tag{14}$$

Sufficiently close to the critical region, the two-dimensional nature of Eq. (14) is expected to be unimportant, because dissipation due to the friction contracts the SQUID dynamics into a one-dimensional manifold. In fact, a function $z=z(\theta,\dot{\theta})$ exists, such that the mapping $z_{n+1}=h(z_n)$ is strictly one dimensional, but it is quite difficult to determine $z(\theta,\dot{\theta})$. However, since here universality is essentially a one-dimensional property, we may also approximate Eq. (13a) through

$$\beta_C\dot{\theta}((n+1)T_D)=g(\dot{\theta}(nT_D))+\xi(n)\ . \tag{15a}$$

Here the noise possesses the following distribution (T_D is the period of the driving flux):

$$P(\xi(n))\sim\exp\left[-\frac{I_c\phi_0\xi(n)^2}{4\pi k_BTT_D}\right]\ . \tag{15b}$$

As seen in the return map in Fig. 8 for the internal flux, the one-dimensional approximant leads, in general, to a multivalued function g. However, sufficiently close to the point of tangential contact, the approximation remains valid, and we therefore expect the intermittency that we have found in SQUID's to belong to the same universality class with the mapping (11), with the appropriate value for z. Therefore, the scaling laws (12a) and (12b) are also applicable.

It is interesting to note that just prior to the onset of intermittency, the laminar time scales with temperature as follows:

$$t_{\rm lam}\sim\sigma^{2(1-z)/(1+z)}\sim(k_BT)^{-1/3}\ \text{ for } z=2\ . \tag{16}$$

This is obtained by allowing σ and $\epsilon\to0$, such that $\sigma\sim\epsilon^{(z+1)/2z}$, and by applying the scaling equation (12b). The scaling law is a new and remarkable behavior, which is also potentially observable. In particular, it is quite manifestly different from the usual well-known behavior of the flux uncertainty in a quasistationary strongly damped SQUID. For the latter case, Kurkijärvi[23] obtained the lifetime of the zero-flux-quantum state to be equal to

$$t_{\rm lam}=\int_{t_0}^{\infty}dt\,t\exp\left[-\int_{t_0}^{t}dt'\frac{R\omega^2(t')}{2\pi}\times\exp\left[-\frac{\Delta U(t')}{k_BT}\right]\right]\ , \tag{17}$$

where $\Delta U(t)$ is the height of the potential barrier between the one- and zero-quantum states at time t, and $\omega(t)$ is the resonance frequency of the zero-quantum state in which the system is prepared at the initial time t_0.

Chaotic time evolution observed in an experiment could be due to both external or internal noise sources. In order to determine which one of these is relevant, it is necessary to determine an equivalent noise temperature for the intrinsic chaos, as in Ref. 10. We equate the noise temperature T_n with the temporal average of the kinetic energy of the chaotic motion as follows:

$$k_BT_n=\tfrac{1}{2}\left\langle C\left[\frac{d\phi_{\rm chaotic}}{dt}\right]^2\right\rangle_{\rm av}\ . \tag{18}$$

In dimensionless units this yields

$$k_BT_n=\tfrac{1}{2}C\left[\frac{\hbar}{2e}\right]^2\omega_J^4(RC)^2\omega_{res}\langle\,|\,\dot{\theta}(\omega)\,|^2\rangle_{\rm av}\ . \tag{19}$$

For the SQUID parameter values quoted in Sec. II, this gives the estimate $T_n=200$ K. Therefore, the noise rise due to intermittency is certainly expected to be an observable phenomenon in a SQUID at the liquid-helium temperatures. However, one should observe that the noise temperature depends quadratically on the critical current and the resistance of the junction, while the dependence on the capacitance is linear. The values of these parameters vary over some two decades between different SQUID magnetometers. In designing experiments on chaos in SQUID's, proper consideration of the effective noise temperature must be taken into account.

IV. FEIGENBAUM SEQUENCES IN rf SQUID's

Sequences of period doublings have been observed both in externally driven and in autonomous dynamical systems. Mathematically, this is a very well understood route to chaos. Under quite general conditions the se-

quence is universal: asymptotically independent from the specific system under consideration, as the control parameter approaches the value at which fully developed chaos appears. The period-doubling route is characterized by the critical exponents δ and α, defined as follows:

$$\lim_{i\to\infty}\frac{\mu_i-\mu_{i-1}}{\mu_{i+1}-\mu_i}=\delta \tag{20a}$$

and

$$\lim_{i\to\infty}\frac{C_i}{C_{i+1}}=\alpha\ . \tag{20b}$$

Here μ_i and C_i, respectively, are the values of the control parameter and the amplitude of the bifurcation branch between the ith and the $(i+1)$th bifurcation for a fixed stability.

The actual numerical values of these critical exponents depend on the universality class for the particular system: the nature of the maximum of the return map and whether the dynamics is conservative or dissipative. The well-known logistic mapping

$$\theta_{n+1}=\lambda\theta_n(1-\theta_n),\quad \theta_n\in[0,1] \tag{21}$$

features a quadratic maximum and is dissipative. The critical exponents for the logistic dynamics[21] are the well-known Feigenbaum numbers $\delta=4.6692\ldots$ and $\alpha=2.5029\ldots$.

The reflection symmetry of the effective potential in Fig. 4 prohibits the appearance of a simple Feigenbaum sequence when starting from the oscillatory zero-quantum state.

Levinsen[14] and later Elgin *et al.*[24] showed, by considering the Duffing oscillator, that provided the potential has even parity under the change of sign of θ, it is impossible to have a symmetric solution with a period twice the period of the drive field. The linear stability of the simple limit cycle $(\omega=\omega_D)$ $\theta_0(\tau)$, is governed by the Hill's equation:

$$\beta_C\delta\ddot{\theta}+\delta\dot{\theta}+\frac{1}{\beta_L}\delta\theta+\delta\theta\cos\theta_0(\tau)=0\ .$$

Linear differential equations with periodic coefficients may have instabilities of period equal to or twice that of the coefficients.[25] If $\theta_0(\tau)$ is not symmetric, the frequency of the coefficient is ω_D, and thus period-doubling linear instabilities may occur. However, for a symmetric $\theta_0(\tau)$ the frequency of $\cos\theta_0(\tau)$ is $2\omega_D$ and no linear subharmonic instabilities exist. Higher-order subharmonics appear discontinuously and coexist with the simple solution. Furthermore, they need not be symmetric, and hence Feigenbaum sequences containing frequencies $\omega_n^{(m)}=\omega_D/2^n(2m+1)$ may appear. If the limit cycle breaks the symmetry of the potential spontaneously, a pure Feigenbaum sequence (with $\omega_n=\omega_D/2^n$) is possible.

The period-doubling cascade is observable in SQUID's. We have described some of the features of this sequence for $\omega_D=\omega_{\rm res}$ in the first report.[16] Further data obtained for other values of the drive frequency ω_D have completed the picture. The main properties of the Feigenbaum sequences in SQUID's may be summarized as follows.

(i) The 2^n sequences appear in a gap between the two split chaotic subbands which correspond to the same n-quantum process. The sequences are encountered on both increasing and decreasing the amplitude A. These regions are separated by values of amplitude for which a period-one limit cycle is stable.

(ii) Some period-doubling cascades with periods $(2m+1)2^n$ were found in small regions at the high-frequency part of the phase space. These chaotic bands are disconnected from the main bands.

(iii) In agreement with the conclusions of Levinsen[14] and of Elgin *et al.*,[24] we did not find any symmetric 2^n period-doubling cascades. The main chaotic band was ap-

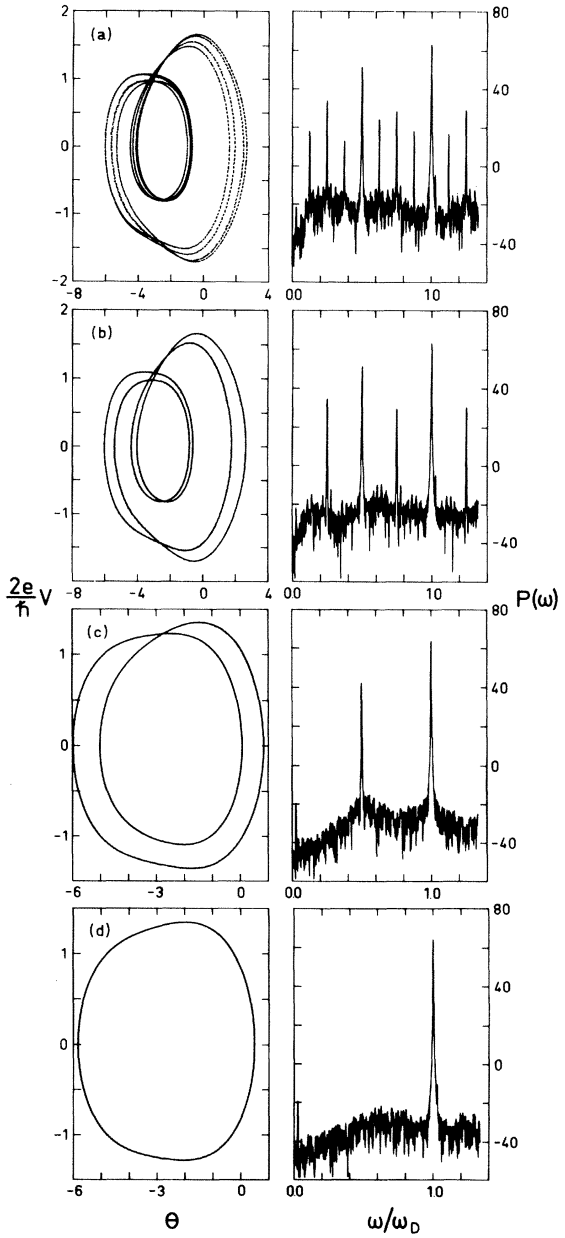

FIG. 9. Lissajous figures and the corresponding power spectra at $\omega_D=\omega_{\rm res}$ for a sequence of bifurcating orbits exemplifying a Feigenbaum period-doubling cascade as a function of the control parameter A. (a) $A=67.65$; (b) $A=68.0$; (c) $A=72.0$; (d) $A=75.0$.

proached intermittently from the symmetric orbits.

(iv) The critical exponents δ and α agreed with the Feigenbaum constants for the logistic equation within the precision of the computation (four to five first bifurcations). It appears that chaos in the symmetry-broken regimes of the phase space is well described by a return map with a quadratic maximum (see also, Fesser, Bishop, and Kumar in Ref. 17).

A sequence of bifurcating nonsymmetric orbits is displayed in Fig. 9. Also, the subharmonic power spectra are given. Figure 10 presents a multifurcation tree for $\omega_D=\omega_{\rm res}$, including the range of Fig. 9.

Note that at the low-frequency side of the one-flux-quantum bands, an interesting point exists at which regions of intermittent and period-doubling chaos merge together. However, no crossover effects occur around this point since a line of discontinuous transition, the breaking of the symmetry of the potential, necessarily passes through the same point.

In conclusion, the period-doubling route to chaos is an important source of intrinsic noise in weakly damped SQUID's driven at a high frequency. An essential noise rise is observed down to $\omega_D=0.25\omega_{\rm res}$, the lowest frequency for which we have performed computations in this paper (at low frequencies the numerical calculations become very time consuming if high accuracy is needed, due to the presence of vastly different time scales in the system). The period doublings are easily distinguished from intermittency due to the simultaneous appearance of the dc magnetization. Also, a strong subharmonic half-frequency peak is observed in the power spectrum, whereas the intermittent spectra are broad and featureless.

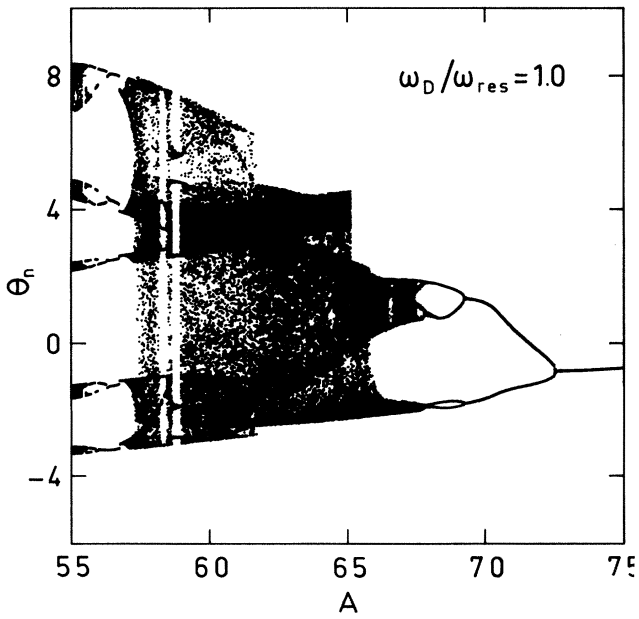

FIG. 10. Multifurcation tree diagram for the phase difference θ of the order parameter as a function of the drive amplitude A at $\omega_D=\omega_{\rm res}$. Shown are the period-5 region, the chaotic regime with windows of phase-locked limit cycles, and the reverse Feigenbaum sequence. Note that in the range $A=55.0$ to 57.1, two reflection-symmetric solutions of period 5 exist, and their basins of attraction move in such a manner that the initial conditions used in the present paper $[\theta(\tau=0)=\dot\theta(\tau=0)=0]$ alternate between one and the other.

External noise due to thermal excitation produces two kinds of effects on the period-doubling sequence. (i) In Sec. II we discussed the thermally activated transitions between the two nonsymmetric limit cycles. This effect is nonuniversal in that it is determined by the basins of attraction. (ii) A universal thermal noise effect arises from the uncertainty in determining the period-doubling structure. As soon as the fluctuations in the voltage due to thermal motion become comparable to the width of the bifurcation branch, the fine structure of the cascade is unobservable. Crutchfield *et al.*[26] have discussed effects due to both additive and parametric noise in the logistic equation. Smoothing in the dependence of the Lyapunov exponent on the control parameter and in the attractor distribution function was found. The most striking feature is the appearance of a gap in the bifurcation sequence: Only the periods with frequency $\omega_n=\omega_D/2^n$ with $n<n_0$ are seen before thermal motion washes out further subharmonics. This is understandable in the framework of the scaling picture by noting that the subharmonic peak in the power spectrum corresponding to a $\omega_D/2^{n+1}$ component lies 13.6 dB below that of a $\omega_D/2^n$ component.[27] Hence for sufficiently large n_0, the intrinsic subharmonic peaks at $\omega_D/2^{n_0}$ lie below the external noise level.

Following the derivation preceding Eqs. (15), we may again formally construct a one-dimensional return map for the SQUID dynamics. We assume that as far as the bifurcation properties are concerned, this mapping is well approximated by the logistic equation with additional noise, and is appropriately scaled. Crutchfield *et al.*[26] have presented the numerical result that for $\sigma=10^{-2}$, the few first bifurcations are observable. Thus

$$\frac{2\pi k_B T}{I_c\phi_0\Lambda^2}T_D<10^{-4}\,, \tag{22}$$

where Λ is the scaling factor which reduces the return map to be defined on [0,1]; it approximately equals 4. This yields the temperature limitation

$$T\lesssim 100\ \text{mK}\,. \tag{23}$$

This is the most stringent restriction for the experiment. This temperature depends linearly on the critical current I_c in the junction. All the noise considerations favor large values of the critical current.

Yet, another source of experimental difficulties must be considered. A small dc term in the external flux breaks the symmetry of the potential, and thus allows a solution with frequency $\omega_D/2$. The basin of stability of this solution has not been considered here. Arguments parallel with those in Sec. II lead to the conclusion that in an experiment the small symmetry-breaking field would not significantly change the above results.

V. rf POWER ABSORBED IN CHAOTIC SQUID's

The resonance frequency [Eq. (6)] of the rf SQUID equals $\omega_{\rm res}=0.8\times10^{11}$ Hz for the parameter values quoted in Sec. II. It is quite difficult, if not impossible, to detect such a rapidly oscillating magnetic field with the

use of an inductively coupled tank circuit. Here we suggest two different measurements to investigate the chaotic SQUID dynamics: (i) detection of the far-infrared or radio-wavelength signal emitted by the SQUID (ω_{res} corresponds to 0.5-mm wavelength), and (ii) determination of the interesting signatures of the nonlinear dynamics (bifurcation points, onset of chaos, etc.) in the power losses of the external field. In both of the above cases a radiation field propagating along a waveguide to the SQUID is the most suitable way of providing the external high-frequency field. In this section we discuss the power-loss method, since we find it more practical and its use requires some new results. The hysteretic behavior of SQUID's driven at a low frequency was discussed in the Introduction, although we did not consider the effects due to external noise sources.

The electromagnetic energy absorbed per cycle (i.e., the average area of the hysteresis loop) is calculated here as a function of the amplitude of the driving field for the three representative values of the drive frequency, $\omega_D/\omega_{res}=0.25$, 0.5, and 1.0. The results are illustrated in Figs. 11—13. The strong contrast between these graphs and the corresponding quasistationary one in Fig. 3 is apparent. The staircase structure of Fig. 3 is smoothened, except for the initial discontinuous transition to the lower two-flux-quantum subband at $\omega_D=0.25\omega_{res}$. Detailed fine structure is observed, most distinctly for $\omega_D=0.5\omega_{res}$. The principal reason for this is the different dependence on drive amplitude of the energy absorbed by the subharmonic orbits. By a comparison of Figs. 11—13 with Fig. 5(a), we deduce the following systematic patterns of behavior.

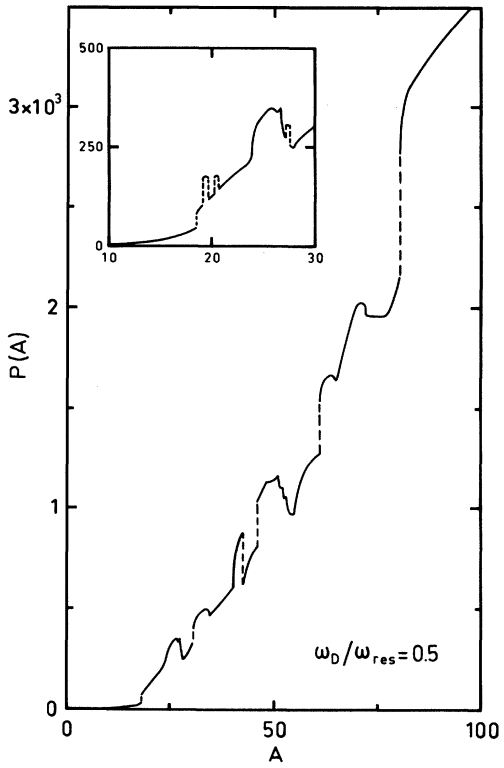

FIG. 12. Same as in Fig. 11, but for $\omega_D=0.5\omega_{res}$. Note the discontinuities marking the intervals of phase-locked solutions within chaotic bands.

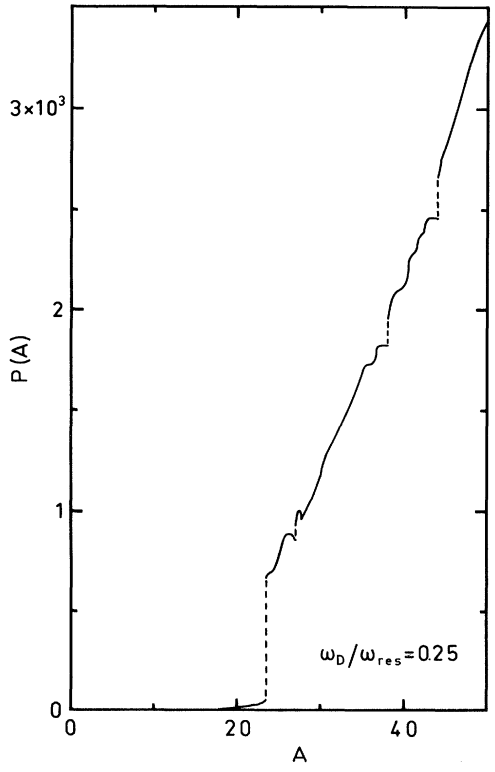

FIG. 11. Averaged energy $P(A)$ absorbed by the rf SQUID per unit cycle of the drive at $\omega_D=0.25\omega_{res}$ as a function of the amplitude A.

(i) The power absorbed in hysteretic period-2 orbits illustrated in Fig. 14(a) decreases with increasing amplitude.

(ii) The 2^n orbits with $n\geq 2$ absorb more energy for increasing drive amplitudes, but at the points of bifurcation we find discontinuities in the slope of $P_{hyst}(A)$.

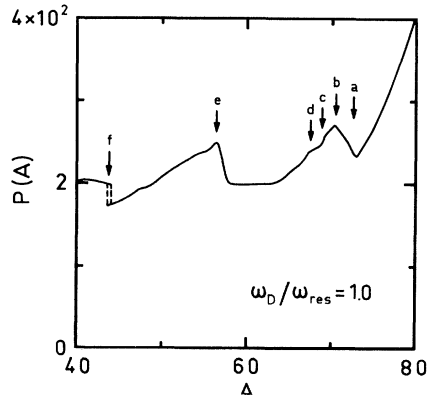

FIG. 13. Same as in Fig. 11, but for $\omega_D=\omega_{res}$. The arrows marked a, b, and c point out the first three bifurcations of the Feigenbaum sequence (cf. Fig. 10). The onset of period-doubling chaos is denoted by d, while e indicates the onset of intermittent chaos. At f the initial conditions used oscillate between the basins of attraction of the phase-locked period-1 and period-5 solutions.

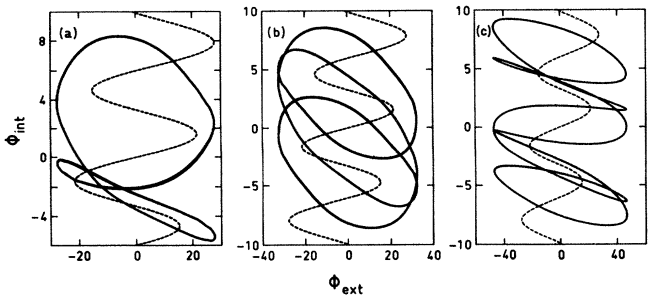

FIG. 14. Internal flux ϕ_{int} as a function of the external sinusoidally varying flux ϕ_{ext} (both in units of $\phi_0/2\pi$) for typical subharmonic solutions. (a) Period-2 solution at $\omega_D=0.5\omega_{res}$ and with $A=27.8$; (b) period-3 solution with $\omega_D=0.5\omega_{res}$ and $A=32.5$; (c) period-5 solution for $\omega_D=\omega_{res}$ and $A=47.0$. Increasing the amplitude of the drive in (a) elongates the loops, but since the orbit must approach the period-1 motion simultaneously (reverse Feigenbaum sequence), the larger loop gets thinner, and hence the overall area traversed by the cycle (i.e., power absorbed in the hysteresis) decreases, in agreement with Figs. 11–13.

(iii) The period-3 orbits behave in a manner similar to those with period 2^n, but are distinguishable from the latter in that no dc magnetization appears in connection with a period-3 orbit, such as the one shown in Fig. 14(b).

(iv) During a period-5 orbit such as the one in Fig. 14(c) (and in the intermittently chaotic trajectory entered from a period-5 orbit), the SQUID absorbs essentially no more energy than in the course of the simple zero-quantum orbit.

(v) Since the time interval between the emissions (or absorptions) of the flux quanta equals $t=t_{0\text{-quantum}}+t_{1\text{-quantum}}$, and thus according to the scaling theory of intermittency $t=C\mid A-A_c\mid^{-(1-1/z)}+D$, one would expect $P_{hyst}(A)$ to start increasing as $(A-A_c)^{(1-1/z)}$. We encountered very rapid growth, which is indicative of a discontinuity; we do not have an explanation for this behavior.

(vi) For $\omega_D=0.5\omega_{res}$, some points of discontinuity in $P_{hyst}(A)$ are quite distinct. These correspond to phase-locked limit cycles (or "commensurable" states) inside the mainly chaotic subbands, and are similar in character to the partial jumps observed in Josephson junctions.[28] The latter have been interpreted by Høgh-Jensen *et al.*[29] in terms of phase lockings in the framework of the circle mapping. Judging from these results, we expect a detailed fine structure to also be found within the chaotic bands of the SQUID.

We suggest experiments to verify the above predictions. The drive frequency $\omega_D=0.5\omega_{res}$ is especially interesting. We want to emphasize that the critical exponent of the period-doubling sequence, δ, and that of intermittency, z, can be obtained from such experiments. The great advantage of the present approach is that only dc measurements are required. Therefore, we suggest similar considerations to be carried out in connection with the current-driven Josephson junction as well.

The results in Figs. 11–13 were obtained in the absence of thermal noise. The conclusions discussed in Secs. III and IV, concerning the limitations of temperature and the dc offset term, are expected to remain valid for the considerations presented in this section as well.

VI. DISCUSSION

We have shown that both the period-doubling and intermittent routes to chaos are encountered in weakly damped hysteretic rf SQUID's, under a strong periodic drive at a high frequency. We have also suggested easily measurable manifestations of these phenomena. Finally, we have considered experimental aspects limiting the observability of these effects due to the presence of thermal noise and an external stray dc-flux term. The most restrictive condition was found to be set by the operating temperature necessary for observing the bifurcation tree. In order to simplify the discussion, all the numerical data presented in this paper are given for fixed values of the McCumber parameters β_C and β_L; changes in these do not qualitatively alter our predictions.

We have omitted from our considerations the small $\cos\theta$ term,[30] whose effects are not qualitatively important, as long as this term will not change the sign of the friction term in the course of an orbit. An example of the opposite case is provided by the Leggett equations, which describe the nonlinear nuclear-spin dynamics in a homogeneous sample of superfluid ^{3}He in the presence of a driving term.[31] However, spatial inhomogeneities are likely to render the simplified damped-pendulum picture of the superfluid spin dynamics suspect.[32] We would therefore expect measurements on nonlinear dynamics with a SQUID ring to be much simpler to perform in practice, than for a macroscopic sample of superfluid ^{3}He. In addition to the rf SQUID considered here, the dc SQUID is interesting in that it provides an autonomous system for nonlinear studies.

Concerning the difficulties that may arise in the experiments, we want to note further that although we have given some estimates for the temperature limitations, more quantitative numerical results in the presence of an external noise are required. We generally neglected the effect of an external dc flux, or reasoned its effects on the structure of the phase space to be minor. However, we conclude that an rf SQUID is an interesting nonlinear device, which shows quite varied chaotic behavior that is readily accessible for experimentation.

Note added in proof. Recently a general proof on the impossibility of periodic doublings out of a symmetric orbit was given [J. W. Swift and K. Wiesenfeld, Phys. Rev. Lett. 52, 705 (1984)]; this should be compared with our findings and, in particular, the discussion below Eq. (21) in this paper and also that in Refs. 14 and 24.

ACKNOWLEDGMENTS

We have benefited from discussions with B. S. Deaver, G. B. Donaldson, and J. Kurkijärvi. One of us (M.M.S.) is supported by the Academy of Finland.

[1]For reviews, see, e.g., J.-P. Eckmann, Rev. Mod. Phys. 53, 643 (1981); A. J. Lichtenberg and M. A. Lieberman, *Regular and Stochastic Motion* (Springer, New York, 1983).

[2]M. J. Feigenbaum, J. Stat. Phys. 19, 25 (1978); 21, 669 (1979).

[3]P. Collet and J.-P. Eckmann, *Iterated Maps on the Interval as Dynamical Systems* (Birkhäuser, Boston, 1980).

[4]J. Maurer and A. Libchaber, J. Phys. (Paris) Lett. 40, L419 (1979); J. Maurer and A. Libchaber, J. Phys. (Paris) Colloq. 41, C3-51 (1980).

[5]J. P. Gollub and S. V. Benson, J. Fluid Mech. 100, 449 (1980); C. W. Smith, M. J. Tejwani, and D. A. Farris, Phys. Rev. Lett. 48, 492 (1982); J. Testa, J. Perez, and C. Jeffries, *ibid.* 48, 714 (1982); C. Jeffries and J. Perez, Phys. Rev. A 27, 601 (1983), and references therein.

[6]Bambi Hu and J. Rudnick, Phys. Rev. Lett. 48, 1645 (1982).

[7]J. E. Hirsch, B. A. Huberman, and D. J. Scalapino, Phys. Rev. A 25, 519 (1982); J. E. Hirsch, M. Nauenberg, and D. J. Scalapino, Phys. Lett. 87A, 391 (1982).

[8]F. M. Izrailev, M. I. Rabinovich, and A. D. Ugodnikov, Phys. Lett. 86A, 321 (1981); J. Frøyland, Physica 8D, 423 (1983).

[9]J. B. McLaughlin, J. Stat. Phys. 24, 375 (1981); R. W. Leven and B. P. Koch, Phys. Lett. 86A, 71 (1981).

[10]R. L. Kautz, J. Appl. Phys. 52, 3528 (1981); 52, 6241 (1981).

[11]R. Y. Chiao, M. J. Feldman, D. W. Peterson, B. A. Tucker, and M. T. Levinsen, in *Future Trends in Superconductor Electronics—1978 (Charlottesville, Virginia),* proceedings of the Conference in Future Trends in Superconductive Electronics, edited by B. S. Deaver, C. M. Falco, J. H. Harris, and S. A. Wolf (AIP, New York, 1978).

[12]B. A. Huberman, J. P. Crutchfield, and N. H. Packard, Appl. Phys. Lett. 37, 750 (1980); see also N. F. Pedersen and A. Davidson, *ibid.* 39, 830 (1981).

[13]D. D'Humieres, M. R. Beasley, B. A. Huberman, and A. Libchaber, Phys. Rev. A 26, 3483 (1982); A. H. MacDonald and M. Plischke, Phys. Rev. B 27, 201 (1983).

[14]M. T. Levinsen, J. Appl. Phys. 53, 4294 (1982).

[15]E. Ben-Jacob, I. Goldhirsch, Y. Imry, and S. Fishman, Phys. Rev. Lett. 49, 1599 (1982); W. J. Yeh and Y. H. Kao, Appl. Phys. Lett. 42, 299 (1983).

[16]R. K. Ritala and M. M. Salomaa, J. Phys. C 16, L477 (1983).

[17]K. Fesser, A. R. Bishop, and P. Kumar, Appl. Phys. Lett. 43, 123 (1983); the rf-SQUID chaos was discussed earlier under linear drive by P. M. Marcus, Y. Imry, and E. Ben-Jacob, Solid State Commun. 41, 161 (1982).

[18]W. C. Stewart, Appl. Phys. Lett. 12, 227 (1968); D. E. McCumber, J. Appl. Phys. 39, 3113 (1968).

[19]O. V. Lounasmaa, *Experimental Principles and Methods Below 1 K* (Academic, New York, 1974), Chap. VII.

[20]Y. Pomeau and P. Manneville, Commun. Math. Phys. 74, 189 (1980).

[21]P. Manneville and Y. Pomeau, Physica 1D, 219 (1980).

[22]J.-P. Eckmann, L. Thomas, and P. Wittwer, J. Phys. A 14, 3153 (1981).

[23]J. Kurkijärvi, Phys. Rev. B 6, 832 (1972).

[24]J. N. Elgin, D. Forster, and S. Sarkar, Phys. Lett. 94A, 195 (1983).

[25]See, e.g., E. A. Coddington and N. Levinson, *Theory of Ordinary Differential Equations* (McGraw-Hill, New York, 1955); Chaps. III and VIII; G. Iooss and D. D. Joseph, *Elementary Stability and Bifurcation Theory* (Springer, New York, 1980), Chaps. VII–IX.

[26]J. P. Crutchfield, J. D. Farmer, and B. A. Huberman, Phys. Rep. 92, 45 (1982).

[27]M. J. Feigenbaum, Phys. Lett. 74A, 375 (1979).

[28]V. N. Belykh, N. F. Pedersen, and O. H. Soerensen, Phys. Rev. B 16, 4860 (1977).

[29]M. Høgh-Jensen, P. Bak, and T. Bohr, Phys. Rev. Lett. 50, 1637 (1983).

[30]A. Barone and G. Paterno, *Physics and Applications of the Josephson Effect* (Wiley, New York, 1982).

[31]Y. Yamaguchi, T. Katayama, and C. Ishii, Phys. Lett. 91A, 299 (1982); T. Katayama, Y. Yamaguchi, F. Furukawa, and C. Ishii, Phys. Rev. B 27, 3096 (1983); Y. Yamaguchi, Prog. Theor. Phys. 69, 1377 (1983).

[32]V.L. Golo and A. A. Leman, Zh. Eksp. Teor. Fiz. 83, 1546 (1982) [Sov. Phys.—JETP 56, 891 (1982)].